USAARL Report No. 99-18

Concept Phase Evaluation of the Microvision, Inc. Aircrew Integrated Helmet System HGU-56P Virtual Retinal Display

By

Clarence E. Rash

Aircrew Health and Performance Division

and

Thomas H. Harding
John S. Martin
Howard H. Beasley

UES, Inc.

August 1999

U.S. Army Aeromedical Research Laboratory
Fort Rucker, Alabama 36362-0577

Notice

Qualified requesters

Qualified requesters may obtain copies from the Defense Technical Information Center (DTIC), Cameron Station, Alexandria, Virginia 22314. Orders will be expedited if placed through the librarian or other person designated to request documents from DTIC.

Change of address

Organizations receiving reports from the U.S. Army Aeromedical Research Laboratory on automatic mailing lists should confirm correct address when corresponding about laboratory reports.

Disposition

Destroy this document when it is no longer needed. Do not return it to the originator.

Disclaimer

The views, opinions, and/or findings contained in this report are those of the author(s) and should not be construed as an official Department of the Army position, policy, or decision, unless so designated by other official documentation. Citation of trade names in this report does not constitute an official Department of the Army endorsement or approval of the use of such commercial items.

REPORT DOCUMENTATION PAGE

Form Approved
OMB No. 0704-0188

1a. REPORT SECURITY CLASSIFICATION
Unclassified

1b. RESTRICTIVE MARKINGS

2a. SECURITY CLASSIFICATION AUTHORITY

2b. DECLASSIFICATION / DOWNGRADING SCHEDULE

3. DISTRIBUTION / AVAILABILITY OF REPORT
Approved for public release, distribution unlimited

4. PERFORMING ORGANIZATION REPORT NUMBER(S)
USAARL Report No. 99-18

5. MONITORING ORGANIZATION REPORT NUMBER(S)

6a. NAME OF PERFORMING ORGANIZATION
U.S. Army Aeromedical Research Laboratory

6b. OFFICE SYMBOL (*If applicable*)
MCMR-UAD

7a. NAME OF MONITORING ORGANIZATION
U.S. Army Medical Research and Materiel Command

6c. ADDRESS (*City, State, and ZIP Code*)
P.O. Box 620577
Fort Rucker, AL 36362-0577

7b. ADDRESS (*City, State, and ZIP Code*)
Fort Detrick
Frederick, MD 21702-5012

8a. NAME OF FUNDING / SPONSORING ORGANIZATION

8b. OFFICE SYMBOL (*If applicable*)

9. PROCUREMENT INSTRUMENT IDENTIFICATION NUMBER

8c. ADDRESS (*City, State, and ZIP Code*)

10. SOURCE OF FUNDING NUMBERS

PROGRAM ELEMENT NO.	PROJECT NO.	TASK NO.	WORK UNIT ACCESSION NO.
62787A	30162787A879	PB	DA336445

11. TITLE (*Include Security Classification*)
CONCEPT PHASE EVALUATION OF THE MICROVISION, INC. AIRCREW INTEGRATED HELMET SYSTEM HGU-56P VIRTUAL RETINAL DISPLAY (U)

12. PERSONAL AUTHOR(S)
Clarence E. Rash, Thomas H. Harding, John S. Martin, and Howard H. Beasley

13a. TYPE OF REPORT	13b. TIME COVERED	14. DATE OF REPORT (*Year, Month, Day*)	15. PAGE COUNT
Final	FROM TO	1999 August	22

16. SUPPLEMENTAL NOTATION

17. COSATI CODES		
FIELD	GROUP	SUB-GROUP
25	03	

18. SUBJECT TERMS (*Continue on reverse if necessary and identify by block number*)
Helmet Mounted Display (HMD), Virtual Retinal Display(VRD), Helmet Gear Unit-56P (HGU-56P), Optical Testing

19. ABSTRACT (*Continue on reverse if necessary and identify by block number*)
In support of the RAH-66 Comanche, Microvision Inc., Seattle, Washington, has developed a prototype helmet mounted display based on laser diode sources. This prototype has been evaluated for optical and visual performance. Tests include: exit pupil size and shape, eye relief, field-of-view, luminance, contrast, contrast transfer function(CTF), modulation transfer function(MTF), and interpupilary distance and vertical adjustments.

20. DISTRIBUTION / AVAILABILITY OF ABSTRACT
☒ UNCLASSIFIED/UNLIMITED ☐ SAME AS RPT. ☐ DTIC USERS

21. ABSTRACT SECURITY CLASSIFICATION
Unclassified

22a. NAME OF RESPONSIBLE INDIVIDUAL
Chief, Science Support Center

22b. TELEPHONE (*Include Area Code*)
(334) 255-6907

22c. OFFICE SYMBOL
MCMR-UAX-SS

DD Form 1473, JUN 86 *Previous editions are obsolete.*

Table of contents

List of figures

Table of contents (continued)

List of figures (continued)

List of tables

Introduction

The program manager, Aircrew Integrated System (PM-ACIS), Huntsville, Alabama, has established a program with Microvision, Inc., Seattle, Washington, to develop a technology demonstrator to determine the capability of a virtual retinal display (VRD) to meet RAH-66 Comanche helmet mounted display (HMD) performance specifications. Under this program, titled Aircrew Integrated Helmet System (AIHS) HGU-56P VRD system, Microvision developed and delivered to the Army a laser based HMD for evaluation by the U.S. Army Aeromedical Research Laboratory (USAARL), Fort Rucker, Alabama. This report constitutes the findings of that evaluation.

The Microvision HMD system is made up of several primary components: an HMD (Figure 1) consisting of a Pilot Retained Unit (PRU) (helmet) and Aircraft Retained Unit (ARU), two Drive Electronics Suites (DES) (Figure 2), interconnect cables, and a Pilot Control Box. The HMD is a binocular optical system custom fitted to a Gentex Corporation, Carbondale, Pennsylvania, HGU-56P aviation helmet. The two DES house the associated electronics, acousto-optical modulators, and power supplies. Fiber optic bundles bring the laser based images to the HMD's optical assemblies that contain high speed microscanners which provide a rastered image via relay optics to the eye. In order to achieve sufficient image resolution (1355 by 960) within the desired frame period, four laser beams are used in parallel to create the image.

The Microvision HMD relay optics include two oculars which are based on a catadiopic design. The oculars consist of dual beamsplitters (Figure 1).

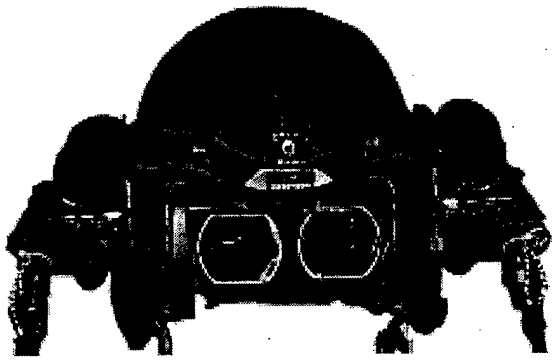

Figure 1. Microvision laser based HMD.

Each side of the HMD had a dedicated laptop computer that provided the video signal (Figure 3). The video fed into the HMD's video interface was a standard computer format of 1280 by 1024 pixels with 8 bits per color at 60 Hz refresh. The HMD displayed only 1280 by 960 of the 1280 by 1024 video image. Only the green 8 bit signal was used to drive the monochrome display. The output from the laptops was further controlled by a main computer that controlled the imagery reaching the HMD.

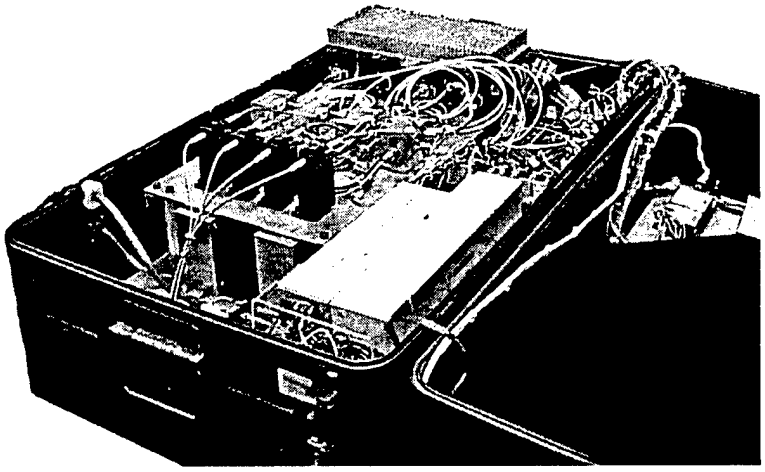

Figure 2. Electronic enclosure for the four lasers, video interface and associated electronics. This enclosure supports one of two optical assemblies.

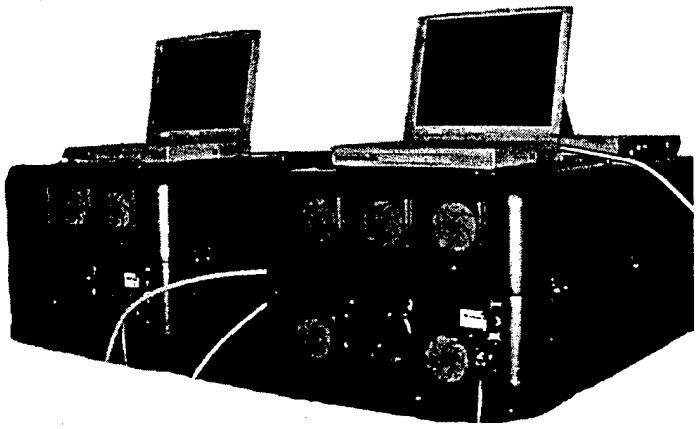

Figure 3. Dedicated laptop image generators providing unique imagery to the two eyes.

System tests

The majority of tests were conducted with the binocular HMD mounted to a rotating stage with the exit pupil from the left or right side centered directly over the center of rotation of the stage (Figure 4). As the stage is rotated in either direction, adjacent imagery comes into view as if seen from a single point in space. Figure 4 shows the video camera and monitor. When the stage is rotated, adjacent pixels come into view in the monitor. In this way, any point along the horizontal axis can be viewed. To evaluate an area that is displaced vertically, the front rod which supports the front of the HMD is raised or lowered. When this rod is raised or lowered, the HMD rotates about an axis which corresponds to a line through the rear bolts which attach the HMD to the two rear posts.

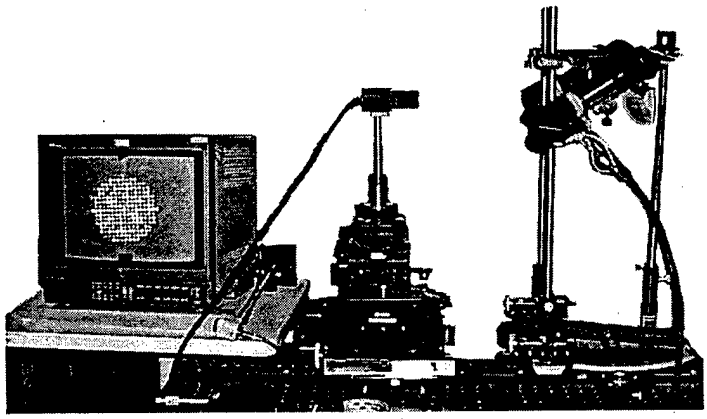

Figure 4. HMD on rotating stage showing camera image of exit pupil.

Exit pupil size and shape

Test equipment: CCD video camera, monitor, computer, image capture card, and millimeter rule.

Test procedure: A grid pattern was displayed on the HMD with the center pixel clearly indicated. The camera was focused to infinity and was aligned with the center pixel of the left or right display. Proper alignment required the center pixel to be in the middle of the monitor with best focus over the entire monitor image. Once proper alignment was achieved, the camera was refocused on the exit pupil (Figure 4), and the HMD alignment image is replaced with a uniform field of high luminance. This image filled the exit pupil with light, and the image of the exit pupil was digitized and stored on a computer for later analysis. With camera focus fixed at the exit pupil, a millimeter rule is imaged on the monitor with the same focal distance and then digitized. This image of the rule provided the basis for calibrated measurements.

Results: Figure 5 shows the exit pupil captured from the left side. Note the small beamletts that make up the exit pupil. These beamletts are the result of the laser projection passing through the exit pupil expander. Comanche requirements specify an exit pupil of 15 mm. Without the exit pupil expander, exit pupil size is approximately 1.3 mm. The exit pupil expander, which is a proprietary item, is in the form of diffractive optics. The laser beam passing through this expander results in multiple beamletts where each beamlett contains the entire displayed image.

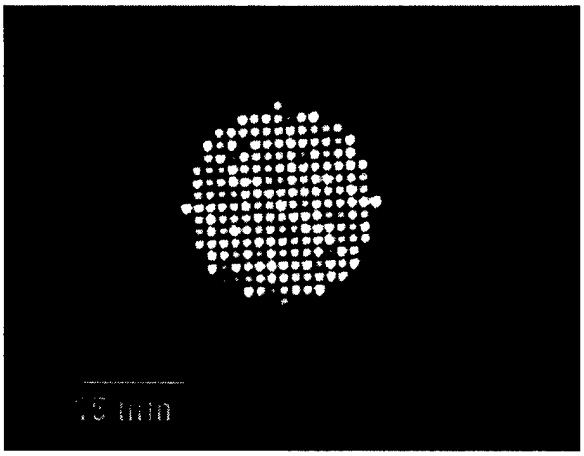

Figure 5. Image of exit pupil captured from the HMD's left side with the camera placed some distance behind the exit pupil (see Figure 4).

Discussion: The horizontal and vertical exit pupil diameter is slightly greater than 15 mm. As can be seen in Figure 5, the exit pupil shape is circular in nature.

Eye relief

Test equipment: Rear projection screen, video camera and monitor, and precision positioners.

Test procedure: A rear projection screen was used to locate the exit pupil position. This was accomplished by moving the rear projection screen along the optical axis until best focus was achieved (Figure 6). Eye relief can be expressed as physical eye relief or optical eye relief. Physical eye relief (eye clearance distance) is defined for the purpose of this report to be the straight line distance from the cornea to the vertical plane defined by the first encountered physical structure of the system. Optical eye relief is the straight line distance from the cornea to the last optical element of the HMD system. In most cases, physical eye relief is much less than optical eye relief and is more relevant in addressing compatibility with life support equipment (i.e., gas mask, oxygen mask, spectacles, etc.). Once the rear projection screen was placed at the exit pupil, a camera mounted on precision positioners was placed to the side in order to observe the distance relationship between the exit pupil and the rear lens in the catadioptic design. By moving the camera laterally, we were able to measure the distance between the rear projection screen and the center and rear edge of the catadiopic design.

Results: Table 1 presents the physical and optical eye relief values.

Table 1.
Physical and optical eye relief (in mm).

	Left side	Right side
Physical eye relief	18.5	19.0
Optical eye relief	39.7	40.5

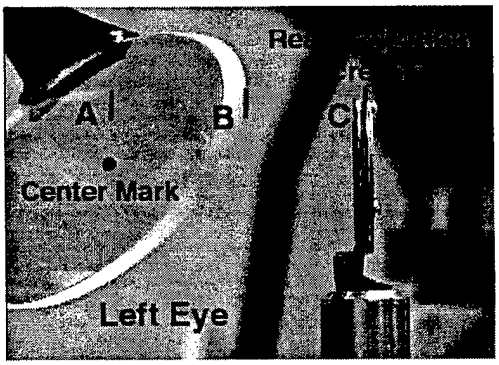

Figure 6. Depiction of optical eye relief (distance A to C) and physical eye relief (distance B to C). The rear screen projection material is collocated at the exit pupil position.

Discussion: At a measured value of 19 mm, the physical eye relief is insufficient for use with a chemical protective mask.

Field-of-view (FOV)

Test equipment: Rotating stage (modified Oriel Model 13038 precision rotating stage), computer and custom software for controlling stage, video camera and monitor.

Test procedure: FOV was measured by rotating the HMD about a point that was fixed at the center of the left or right exit pupil. By ray tracing, it could be demonstrated that the image displayed by the left and right channel were contained within a cone whose apex was at the exit pupil and extended out into space. A video pattern was presented on the display which clearly indicates the horizontal and vertical meridian and the fullest extent of the FOV. To determine horizontal FOV, the camera was set to infinity focus and aligned with the center pixel. When the display was rotated, the horizontal line which marks the horizontal meridian moved along the horizontal axis. At the point where the horizontal line ended, the computer controlled rotator cou;d be polled to retrieve coordinate information. Calculating the coordinates for the two extremes of the horizontal meridian, the horizontal FOV could be calculated. This procedure was repeated for the other side and for the vertical meridian. For the vertical meridian, the HMD must be mounted on its side. To mount the HMD on its side, the two channels were detached from the aircraft retained unit and mounted separately (Figure 7).

Results: Table 2 shows the monocular FOV for each channel.

Discussion: The Comanche requirement of monocular FOV of 30 by 40 degrees is met.

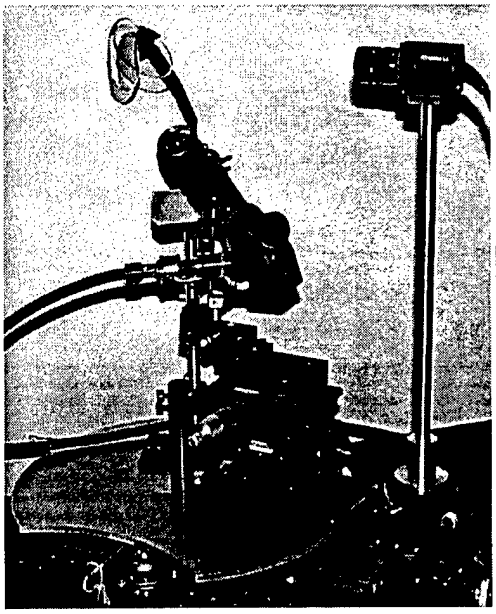

Figure 7. Single channel mounted on rotating stage. Video camera used to measure vertical FOV.

Table 2.
Monocular FOV (in degrees).

	Left side	Right side
Horizontal meridian	40.8	40.2
Vertical meridian	30.1	30.0

Binocular field-of-view and overlap

Test equipment: Chin rest and tangent screen.

Test procedure: The binocular HMD was mounted to its three pole configuration (Figure 4) and a chin rest was mounted such that an observer could see comfortably through the binocular HMD to a tangent screen located a known distance in front. Following the adjustment of the interpupilary distance (IPD) to provide full FOV in each eye, a pattern was displayed that clearly marked the middle of the display and the top, bottom and edges of each monocular FOV. For each channel, the four extremity positions plus the middle position were then plotted on the tangent screen by having the observer guide an assistant in the placement of pins on the board which corresponded to the FOV positions. Using trigonometry, the binocular FOV and overlap were calculated.

Results: The results are shown in Table 3.

Table 3.
Binocular FOV (in degrees).

	Mapping data	Optical data	Percent difference
Left horizontal FOV	39.8	40.8	2.5
Left vertical FOV	29.8	30.1	1.0
Right horizontal FOV	39.6	40.2	1.5
Right vertical FOV	29.5	30.0	1.7
Binocular horizontal FOV	52.1	---	---
Binocular horizontal overlap	26.0	---	---

Discussion: The FOV values collected in this fashion are consistently lower that the values collected optically. We place more confidence in the optically collected data. However the 26 degree overlap is significantly lower than the expected 30 degree overlap required by Comanche.

Binocular alignment

Test equipment: Laser, collimated night vision goggle (NVG) test device from the NVG Test Set (TS-3895A/UV), tangent screen.

Test procedure: A laser projected into one side of the collimated NVG test device produced a second laser beam parallel to the first with the distance separating the two beams equal to the IPD. Having two parallel laser beams allowed testing of the see-through alignment of the HMD optics. The two laser beams were projected onto a tangent screen and their positions marked. Without moving the laser or collimated test device, we placed the HMD into the optical path such that the beams passed through the HMD's optics. Following proper alignment, the position of the laser beams were plotted on the tangent screen and the HMD's deviation from normal was calculated.

Results: The position of the laser beams with and without the optics in place were within ± 1 milliradian.

Discussion: The binocular alignment was within Comanche specification.

Transmissivity

Test equipment: A RS-12 standard tungsten lamp, a Photo Research PR704 spectrascan, and a computer.

Test procedure: The RS-12 standard lamp was placed in front of the left optical lens assembly with the lamp surface orthogonal to the optical axis. With the lens assembly retracted, down position, a spectral scan of the lamp was made and stored on computer. The lens assembly was then placed in position to intersect the lamp, and the spectral scan was repeated. The second scan was then divided by the first scan to find the attenuation in light due to the HMD optics. These data are then plotted as a transmissivity curve. This procedure was then repeated for the right channel.

Results: The results can be seen in Figure 8.

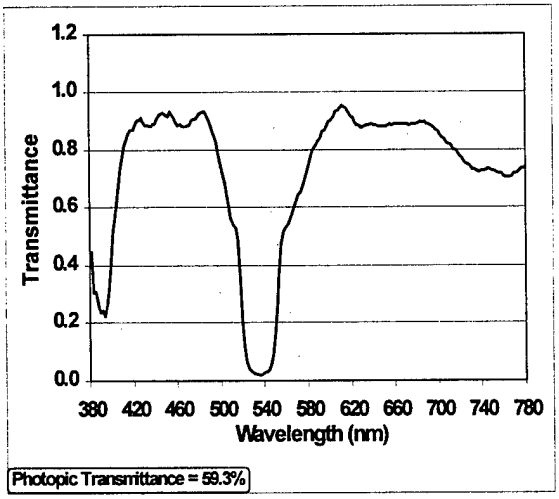

Figure 8. Transmittance of left channel. The large notch near the peak wavelength of the laser is intended to increase reflectance of these wavelengths in order to increase the source luminance reaching the eye. The photopic transmittance (with a tungsten source) is 59.3 percent.

Discussion: Given the high luminance nature of the HMD, the notch bandwidth of 42 nm seems large given the near monochromatic nature of the source. The large notch results in decreased see-through luminance and leads to a degradation in color discrimination and loss of contrast. As a side issue, if P-43 and P-53 phosphors are used in panel mounted cockpit displays, readability of these displays will be significantly reduced by the notch characteristics which are colocated with the peaks of these phosphors.

Spectral output

Test Equipment: Photo Research PR704 spectrascan.

Test Procedure: The spectral distribution of the light output from the HMD was measured using a Photo Research PR704 spectrascan. The PR704 provided a fast scan, and the scan was highly repeatable. The width of the light was only 4 to 5 nm.

Results: The spectral distribution of the light reaching the eye can be seen in Figure 9.

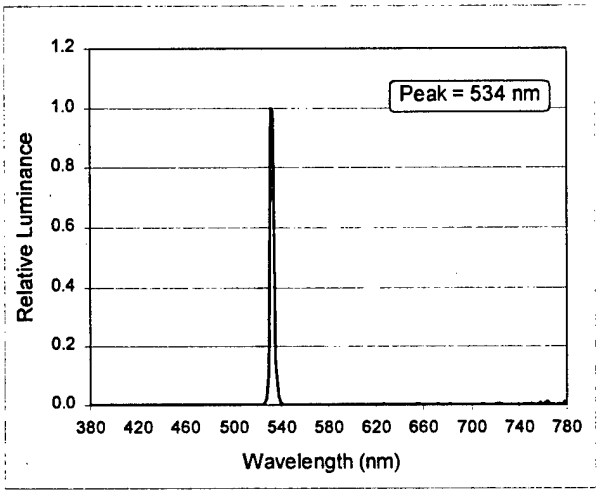

Figure 9. Spectral output of the laser based Microvision HMD.

Discussion: The high monochromaticity is characteristic of laser sources.

Aberrations

Test Equipment: Rotating and translation stages and a calibrated dioptometer.

Test Procedure: An image of a grid pattern with vertical and horizontal lines was presented to a single channel of the HMD at a time. The dioptometer with a 5 mm artificial pupil was placed at the exit pupil. An observer viewed the grid pattern with the dioptometer and focused on the vertical lines and then focused on the horizontal lines. Measurements of the dioptometer's readings were made for each focus adjustment. Field curvature, spherical and astigmatic aberrations were measured for each channel. Field curvature was measured by rotating the HMD about a central axis and taking measurements every 1 degree over the extent of the FOV. Spherical aberration was measured by holding the HMD fixed and translating the dioptometer to either side of the central axis. Measurements could be made to about 7 mm to either side of the central axis due to the size of the exit pupil. The difference between the vertical and horizontal adjustment provided an estimate of spherical aberration.

Results: Aberrations were generally minimal and all were less than 0.5 diopter.

Discussion: The optics were very good and had only minimal optical aberrations.

Luminance response (Gamma)

Test equipment: 1980A Prichard photometer, a Melles Griot integrating sphere and optical power meter.

Test procedure: To measure the Gamma, a 41 pixel square target in the middle of the display was turned on and set to a gray level of from 0 to 255 in about increments of 3. The photometer was focused to infinity and aligned with the middle of the square. A reading was made for each of the gray level settings. For maximum luminance, the entire display was set to a gray level of 255 and an integrating sphere was placed at the exit pupil position in order to capture the entire light output of the HMD. The power measured by the integrating sphere was measured by the optical power meter. Using the luminance efficiency of the peak wavelength of the laser, the luminance at the eye was calculated.

Results: Results are shown in Figure 10. The two curves are compressive with the right side showing slightly better linearity than the left side. Maximum luminance for the left and right side was 808 and 1,111 fL, respectively.

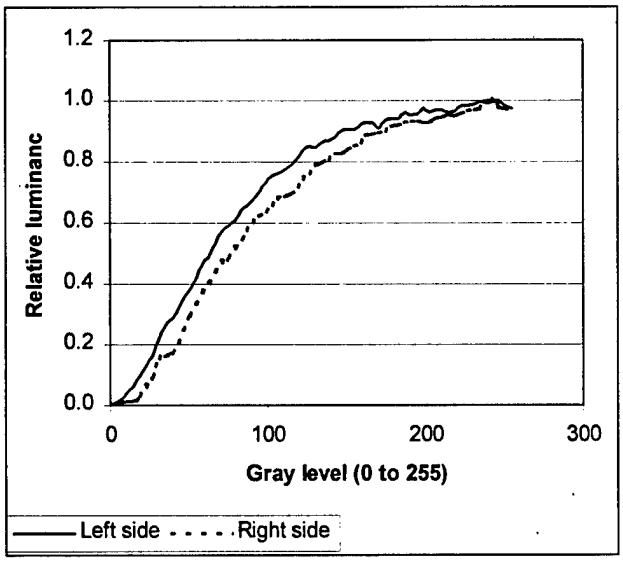

Figure 10. Relative luminance response curves.

Discussion: The Gamma curves were compressive but essentially monotonic in nature. The advantage of this HMD is its high luminance output. Our measurement of absolute luminance was slightly lower that what we witnessed at the Microvision facility. However, during setup at USAARL, it was determined that luminances between channels were not balanced. Subsequent adjustments to laser outputs most likely explain the difference.

Luminance uniformity

Test equipment: Photo Research 1980A photometer.

Test procedure: A 25 square pattern (each square 80 by 64 pixels with a gray level of 255) was presented with the background set to a gray level of 0. The squares were distributed over the viewing area according to the scheme shown below. The luminance of each square was measured in the middle with a 20 arc minute aperture.

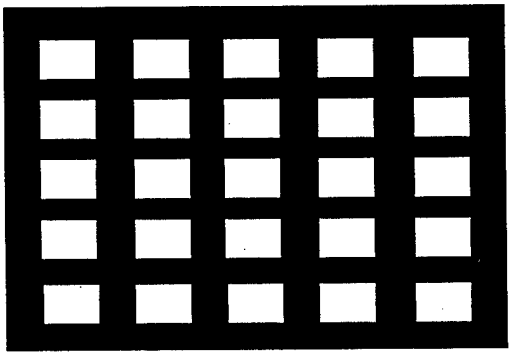

Results: The luminance uniformity results can be seen in Table 4. The measurements are given as a percent of the mean luminance. Note that most squares are within ± 20 percent with the exception of four of the squares.

Table 4.
Luminance uniformity (percent of the mean).

109.79%	97.97%	93.54%	100.43%	128.99%
106.34%	88.62%	91.08%	94.53%	120.62%
100.43%	87.63%	88.13%	99.45%	119.14%
104.37%	96.99%	98.46%	100.43%	127.51%
93.54%	77.79%	80.74%	84.19%	109.29%

Discussion: The uniformity was rather good although 4 of the 25 squares fell outside of the Comanche specification of being within ±20 percent deviation from the mean.

Contrast

Test equipment: 1980A Prichard photometer.

Test procedure: Contrast/contrast uniformity was measured using the same 25 bright square pattern as shown above (Luminance Uniformity section). Contrast ratios were measured using two methods. Peak luminance was measured in the middle of each of the 25 squares. The peak was calculated against the background luminance measured to the side of display (100 pixel distance from the middle or from the bottom of the square (64 pixel distance from the middle).

Results: Table 5a and b show the contrast ratios for the lateral and vertical contrast respectively.

Table 5a.
Lateral contrast ratios.

11.74	13.54	13.97	16.45	20.31
16.00	12.86	14.23	14.01	24.02
16.72	14.71	16.57	18.88	28.47
14.52	12.96	12.58	14.37	21.58
23.46	20.00	21.03	19.43	32.65

Table 5b.
Vertical contrast ratios.

16.52	14.11	12.67	13.78	20.31
14.90	11.18	10.57	11.64	18.28
12.75	10.41	10.78	12.55	19.84
16.96	14.07	12.05	16.19	24.21
31.67	21.94	18.64	20.60	30.41

Discussion: Despite rather good luminance uniformity, the contrast uniformity varied significantly ranging from a minimum of 10.41 to a maximum of 32.65. Contrast uniformity could be improved although there is no Comanche specification for this parameter.

Contrast transfer function (CTF)

Test equipment: 1980A photometer with slit aperture.

Test procedure: Grill patterns (vertical square wave gratings) of increasing spatial frequency were used to measure the CTF. Using a slit aperture aligned with the vertical lines of the grill pattern, the slit traversed the pattern measuring luminance over two cycles of the grill pattern. The luminance of the grill pattern was sampled 32 times in all (16 measurements per grill cycle). Spatial frequencies ranged from 20 to 640 cycles per display width in octave increments (0.5 to 16 cycles/deg). Due to a slow vertical drift present in the imagery, we were only able to measure the CTF in the horizontal axis.

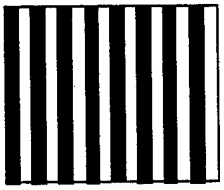

Results: The luminance profiles of the six spatial frequencies are shown in Figure 11. The curves in this figure are labeled according to the number of pixel columns that are off and on in the grill pattern. Calculating the Michaelson contrast from these data, the preliminary CTF is plotted in Figure 12. Michaelson contrast is defined as $(L_{max} - L_{min})/(L_{max} + L_{min})$. Visually observing the highest two spatial frequencies under magnification, we failed to notice any significant luminance modulation. Clearly the luminance profiles for these frequencies failed to show a modulation pattern at 2 Hz and therefore we suspected that the fluctuations were due to noise. To verify this notion, we measured again the luminance profiles at the highest two spatial frequencies. These data are also plotted in Figure 12. The differences were notable and pointed to noise being the probable cause of the discrepancy. In an attempt to accurately portray the CTF for this display, the data in Figure 11 and the repeat measurements were Fourier analyzed in order to determine the actual contrast modulation at the sampled 2 Hz harmonic. The harmonic data are plotted in Figure 13 and these data are likely to be a closer approximation to the true CTF than the data shown in Figure 12. Note that amplitude of the two highest frequencies is essentially the same for the original and repeated measurements.

Discussion: The CTF is rather poor. At the Nyquist frequency (approximately 16 cycles/deg), the contrast was essentially nill. At half the Nyquist frequency, only about 10 percent contrast was achievable. The horizontal grill CTF should provide slightly higher contrast modulation at these higher frequencies since the grill is constructed of single scanned lines. However, due to the vertical drifting problem, this could not be measured using our scanning technique.

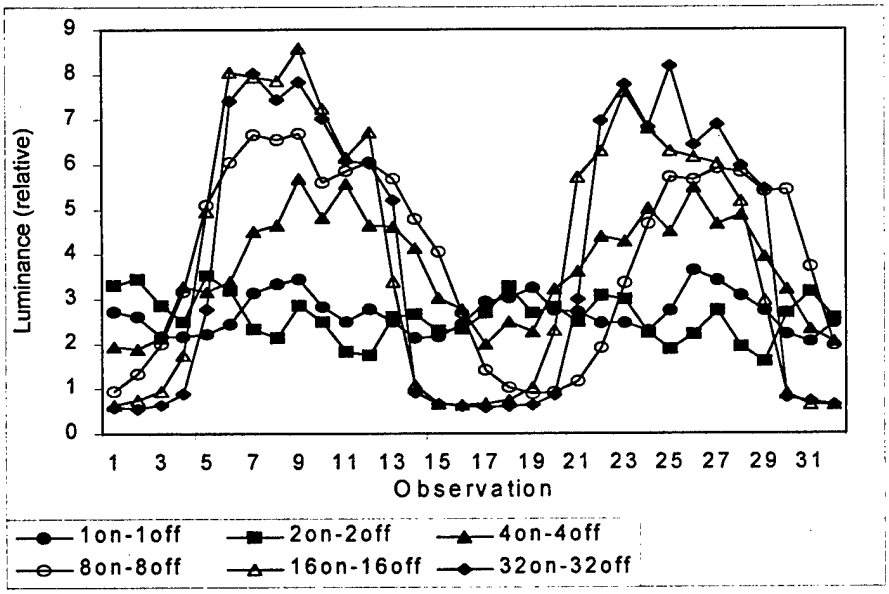

Figure 11. Horizontal luminance profiles of the six spatial frequencies used for the CTF measurement (left side). Note that there is little modulation for the two lowest frequencies.

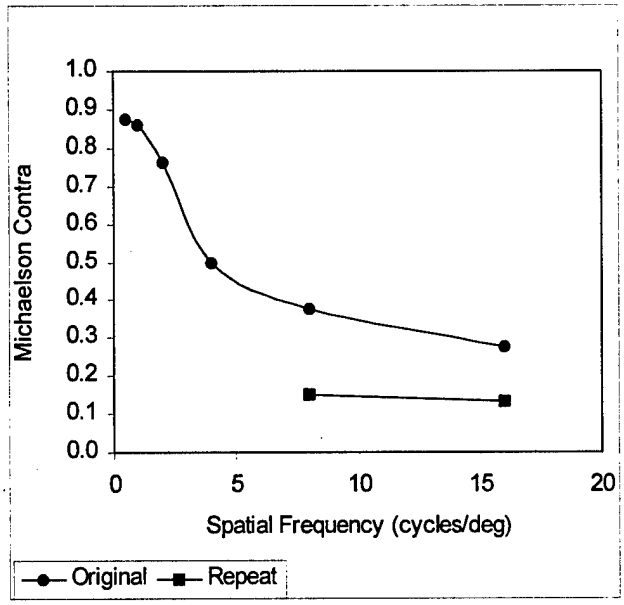

Figure 12. Calculated CTF from the data shown in Figure 11 and repeat measurements of the highest two frequencies.

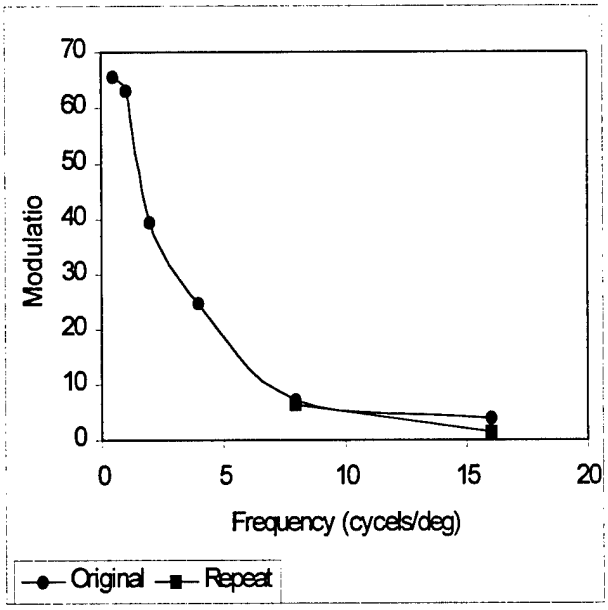

Figure 13. Contrast modulation of the 2 Hz harmonic seen in Figure 11. Notice how the repeat measurements at the two highest spatial frequencies nicely overlap the previous measurements.

Modulation transfer function (MTF)

Test equipment: 1980A Pritchard photometer with a slit aperture and a 25X lens.

Test procedure: A single vertical line in the middle of the display was scanned horizontally with the photometer's slit aperture. The line was scanned in approximate 0.5 arc minute steps for a total of 128 independent measurements. The resulting line spread function was frequency transformed and the normalized MTF calculated. The horizontal line spread function could not be measured using our scanning technique due to the vertical drift present in the system.

Results: The MTFs for the left and right sides are shown in Figure 14. Please note the relatively low modulation at the higher frequencies noted earlier in the CTF measurements.

Discussion: The MTF had a faster roll-off than Comanche specifications dictate.

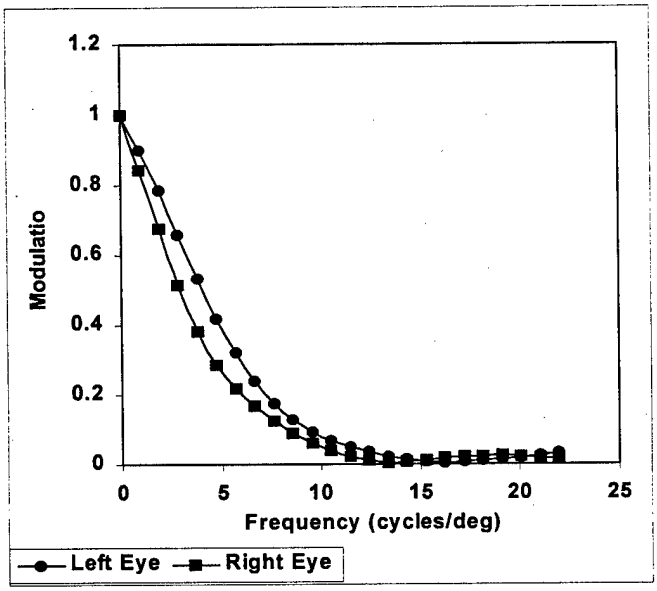

Figure 14. Horizontal MTFs based upon the left and right side vertical line spread functions. Note the low modulation at 16 cycle/deg.

Interpupilary distance (IPD) and vertical adjustments

Test equipment: Exit pupil location device consisting of a section of rear screen projection material sandwiched between circular metal clamps, optical assembly with clamps and rod and a millimeter rule.

Test procedure: Both optical channels were centered. The positions of the left and right exit pupils were found using the rear projection screen. The distance between the two positions was measured. The maximum IPD was measured as a function of the vertical adjustment. To measure the vertical alignment, a marker was placed on the combiner lens assembly which allowed measurement of the vertical extent with a millimeter rule.

Results: The eyepieces could be moved up and down over a 10 mm range. The IPD scale reads 58 to 74 mm, but the range of motion will not extend out to 74 mm. We measured the IPD range to be 57 to 73 mm.

Discussion: The vertical travel and IPD range appear sufficient.

See-through color discrimination

Test equipment: Dvorine Pseudo-Isochromatic plates and a Lanthony's desaturated D-15 hue test.

Test procedure: Three observers with normal color vision were tested using the Dvorine Pseudo-Isochromatic plates and the Lanthony's desaturated D-15 hue test. The Dvorine test consisted of 14 test plates viewed under a MacBeth easel lamp. The observers viewed plates and read the embedded numbers while wearing the helmet mounted display. No more than 5 seconds were allowed per plate. The Lanthony test consisted of 16 color chips (embedded in circular caps) selected from the Munsell Book of Color. The hues (Munsell hues) were selected so that the intervals between different hues were approximately equal. The mean chroma (Munsell chroma) was 2 and the mean luminosity level (Munsell value) was 8. The color caps had scoring values on the bottoms. A reference cap is fixed permanently to the left end of the lower panel of the rack. The remaining 15 caps were placed in random order on the upper panel of the rack. The observers' task was to arrange the color chip caps in order according to color similarity. They were instructed to do this by first locating the color caps that most closely resembled the reference cap and placing it next to it, and then selecting the color cap that most closely resembled the last selected cap, etc., until all of the caps were arranged in order. By closing the rack and turning it over, the scoring numbers became visible and the observer could be scored.

Results: All observers correctly identified the isochromatic plates although with some difficulty. Likewise, the D-15 test was completed successfully by all observers. However, it was noted that the first five chips could be successfully ordered yet they lacked the green tint which would have made the tasking easier.

Discussion: As these tests are designed to catch color discrimination deficiencies based upon cone deficiencies, they may not provide the best measurement of color discrimination deficiencies due to the lens coatings in the HMD. Certainly some discriminations shall be more difficult and this leads to increases in reaction time.

Summary and discussion

Evaluation results are summarized in Table 6. The Microvision laser HMD as a proof of concept was well done and offers many advantages over more mature technologies. The luminance output of this system, although high, fell slightly short of the luminance expectations required by Comanche. In addition, the prototype helmet mockup incorporating this display, while not measured by us, was deemed light weight by observers who have previous experience wearing helmet mounted displays.

The greatest deficiency we noted was the rather poor MTF and CTF. This agrees with observers who noted that the display imagery appeared to be slightly blurred. Possible sources of this MTF/CTF degradation include the exit pupil expander, drive circuits, laser focusing, and possible temporal deficiencies. Luminance uniformity was rather good although several measurements fell outside the ±20 percent Comanche requirement. However, contrast uniformity varied significantly although there is no current Comanche specification for contrast uniformity.

A final area of concern to us was the unsuspected presence of a slow vertical drift in the imagery. The drift had a range of approximately 1 degree visual angle or less. This drift, if uncorrected, could cause major concerns in terms of targeting and tracking performance.

Table 6.
Evaluation summary.

Exit pupil size and shape	Greater than 15 mm and circular
Eye relief	Physical eye relief: 19mm nominally; Optical eye relief: 40 mm nominally
Field-of-view	Slightly greater than 30 by 40 degrees monocularly
Binocular field-of-view and overlap	Horizontal: 52.1 degrees; Vertical: 30 degrees; Overlap 26 degrees
Binocular alignment	Less than milliradian
Transmissivity	Photopic transmission: 59.3% with a tungsten source
Spectral output	Highly monochromatic with a peak at 534 nm
Aberrations	Less than 0.5 diopter
Luminance response (Gamma)	Maximum luminance 1,111 fL; Compressive nonlinearity
Luminance uniformity	16% of area showed greater than ±20% deviation from the mean
Contrast	Contrast was not uniform and ranged from 10.4 and 32.6
Contrast transfer function	Poor high frequency response
Modulation transfer function	Poor high frequency response
IPD and vertical adjustments	IPD range: 57 to 73 mm; vertical range: 10mm

Appendix.

List of manufacturers.

Gentex Corporation
Carbondale, PA 18409

Melles Griot
2985 Sterling Ct.
Boulder, CO 80301

Microvision, Inc.
19910 North Creek Parkway
P.O. Box 3008
Bothell, WA 98011

Oriel Corporation
250 Long Beach Blvd
P.O. Box 872
Stratford, CT 06497

Photo Research
3000 North Hollywood Way
Burbank, CA 91505